Electrochimica Acta 282 (2018) 672–679

Contents lists available at ScienceDirect

Electrochimica Acta

journal homepage: www.elsevier.com/locate/electacta

A cyclic catalysis enhanced electrochemiluminescence aptasensor based 3D graphene/photocatalysts Cu_2O-MWCNTs

Yeyu Wu [a], Xiaoyu Li [a], Xuecai Tan [a, *], Defen Feng [a], Jun Yan [a], Hui Zhang [a], Xiao Chen [a], Zaiyin Huang [a], Heyou Han [b, **]

[a] School of Chemistry and Chemical Engineering, Guangxi University for Nationalities, Guangxi Key Laboratory of Chemistry and Engineering of Forest Products, Key Laboratory of Guangxi Colleges and Universities for Food Safety and Pharmaceutical Analytical Chemistry, Nanning, 530008, China
[b] College of Science, Huazhong Agricultural University, Wuhan, 430070, China

ARTICLE INFO

Article history:
Received 2 April 2018
Received in revised form
9 June 2018
Accepted 14 June 2018
Available online 15 June 2018

Keywords:
Photocatalysts Cu_2O
3D graphene
Multiwalled carbon nanotubes
Electrochemiluminescence
Aptasensor

ABSTRACT

Here, we developed an electrochemiluminescence (ECL) aptasensor for ultrasensitive detection of thrombin (TB) based on a synergistic effect of nanoparticles sensitization and cyclic catalysis of Cu_2O. The aptasensor is constructed from three parts: firstly, three dimensional (3D) graphene was dropped onto the electrode to accelerate electron transfer. Then, the synthesized Cu_2O-multiwalled carbon nanotubes (MWCNTs) were loaded onto the surface of 3D graphene. Finally, after TB aptamers linked to MWCNTs, $Ru(bpy)_3^{2+}$- doped silica nanoparticles (RuSiNPs) were marked onto the surface. When detection of TB, the aptamers folded into G-quadruplex's that made the RuSiNPs get closer to the Cu_2O. As a photocatalysis, Cu_2O was excited by the ECL of RuSiNPs and generated holes and electrons which could catalyze the ECL reaction to emit much light, and the light could excite Cu_2O again. Hence, a cyclic catalytic aptasensor was built. Under the optimal conditions, this aptasensor for TB detection showed good sensitivity with wide linearity (5×10^{-15} M - 5×10^{-11} M) and low detection limit (1.3×10^{-15} M).

1. Introduction

Since 1990, aptamers have been found that can specifically bind to some kind of targets, such as RNA enzymes [1] and organic dyes [2]. Aptamers are single-stranded DNA or RNA oligonucleotides with unique three dimensional structure, that could be used as bio-recognition parts to fabricate selective and sensitive biosensors to detect cells [3], proteins [4,5], ions [6], drugs [7,8], and so on. Compared to antibodies and enzymes, aptamers not only present advantages of smaller size, better thermal and chemical stability, but also can be synthesized in vitro or modified with functional groups which make them as promising sensing parts for bioassay [9]. Up to now, various methods based on aptamer sensors have been widely developed for analysis and detection, such as fluorescence [10], electrochemistry [11], and electrochemiluminescence (ECL) [12,13]. Especially, ECL obtained more attention due to its high sensitivity and selectivity [14–19]. ECL is generated by electron-transfer during electrochemical reactions to form excited states that emit light at specific wavelengths. Tris (2,2′-bipyridyl)ruthenium(II) ($Ru(bpy)_3^{2+}$) is a stable and efficient chemiluminescent reagent that has been widely applied in ECL system. However, $Ru(bpy)_3^{2+}$ is so expensive that using $Ru(bpy)_3^{2+}$ in the solution-phase ECL is not a good deal, so construct solid-state $Ru(bpy)_3^{2+}$ ECL sensor is very important [20–23]. Doping silicon dioxide (SiO_2) nanoparticles has become a popular approach to obtain cost-saving, brilliant, stable biocompatible solid-state ECL sensor. $Ru(bpy)_3^{2+}$–dopped SiO_2 can immobilized $Ru(bpy)_3^{2+}$ firmly by the strong electrostatic interaction, it also can reserve the original electrochemical and luminescent properties of $Ru(bpy)_3^{2+}$ [22,24,25].

Thrombin (TB) is a specific serine protease responsible for blood clotting, and it is also a useful marker which can help diagnose the pulmonary metastasis. As thrombin combines with thrombin aptamer (TBA), the conformation of TBA changes and folds into a unique G-quadruplex structure [26,27]. Up to now, some ECL aptasensors have been built for thrombin detection, including designing affinity aptamers and ECL labels, introducing nanomaterials and designing novel ECL systems [28–35]. However, wider linear ranges or lower detection limits are still great challenges for ultrasensitive detection.

Cuprous oxide (Cu_2O) is one of the most promising semiconductor photocatalysts due to the properties of nontoxicity,

* Corresponding author.
** Corresponding author.
E-mail address: gxunxctan@126.com (X. Tan).

https://doi.org/10.1016/j.electacta.2018.06.104
0013-4686/

stability and ease synthesized [36,37]. Cu_2O is a p-type semiconductor that can be excited by light at 400–800 nm wavelength, and then generate electrons (e^-) and holes (h^+) [38], both of which can catalyze chemical reactions. So $Ru(bpy)_3^{2+}$ generates light at 520–800 nm can excite the Cu_2O, following the produced e^- or h^+ will facilitate the redox reaction of $Ru(bpy)_3^{2+}$ to generate more light, thus the ECL signal will be greatly enhanced. Based on this principle, a cyclic catalysis enhanced system can be built. In addition, carbon materials like multiwalled carbon nanotubes (MWCNTs) can enhance the electron transfer to improve the catalytic capacity of Cu_2O [39]. Similarly, 3D graphene is also a carbon material that possesses a lot of advantages, such as high conductivity, great mechanical strength and large specific surface [40]. 3D graphene not only retains all good properties of 2D graphene, but also has more wrinkles and ripples [41,42]. These excellent characters make it an ideal material to modify electrode [19].

Here, we developed a cyclic catalysis enhanced electrochemiluminescence aptasensor based on 3D graphene/photocatalysts Cu_2O-MWCNTs for thrombin detection. For aptasensor fabrication, 3D graphene used as substrate material to accelerate electron transferred, then Cu_2O-MWCNTs was loaded onto the surface of 3D graphene, finally TBA was linked to MWCNTs and followed by $Ru(bpy)_3^{2+}$ doped SiO_2 nanoparticles (RuSiNPs) was fixed onto the electrode. While detection of TB, the structure change of TBA caused the distance between $Ru(bpy)_3^{2+}$ and Cu_2O became closer, so the cyclic photocatalytic reaction would improve the ECL intensity. The developed aptasensor could specifically and quickly detect thrombin with high sensitivity and wide linear range.

2. Experimental section

2.1. Chemicals and materials

Tris (2,2′-bipyridyl) dichlororuthenium(II) hexahydrate ($Ru(bpy)_3Cl_2 \cdot 6H_2O$), nafion (5 wt%), bovine serum albumin (BSA) and thrombin (TB) were purchased from Sigma-Ardrich (Madrid, Spain). Tetraethyl orthosilicate (TEOS), hexylalchol, N-succinimidyl-4-(N-maleimidomethyl)cyclohexane-1-carboxylate (SMCC), N-(3-dimethyl aminopropyl)-N-ethylcarbodiimidehydrochloride (EDC) and N-hydroxy succinimide (NHS) were purchased from Damas-beta (Shanghai, China). Sodium citrate, L-Asocbric acid (AA) and Copper sulfate pentahydrate were purchased from China national pharmaceutical group corporation (Beijing, China). Triton X-100(TX-100) was supplied by Biosharp (Hefei, China). Graphite powder was offered by Beilian chemical company (Tianjin, China). Hemoglobin (Hb) and Immunoglobulin G (IgG) were purchased from Solabio science and technology Ltd. (Beijing, China). Multiwalled carbon nanotubes (MWCNTs, purity>95%, diameter 20 nm, length 30 μm) were purchased from Chengdu organic chemicals Co. Ltd. (Chengdu, China). Thrombin aptamer (TBA) were acquired from Suzhou hongxun biotechnology Co. Ltd. (Suzhou, China) and has the following sequences:

5′-SH- TCTCTCAGTCCGTGGTAGGGCAGGGTTGGGGTGACT-3′.

Tris–HCl buffer (pH 7.4) containing 140 mM NaCl, 5.0 mM KCl and 1.0 mM $MgCl_2$ was used to dissolve the TBA. Double distilled water (DDW, 18.2 MΩ cm^{-1}) used all throughout the experiments was further purified by the Millipore system.

2.2. Apparatus

The ECL signals were obtained by a MPI-B model electrochemiluminescence analyzer (Xi'an Remax Electronic Science & Technology Co., Ltd., China) with voltage of 800 V provided by photomultiplier tube (PMT). The PGSTAT 128N electrochemical workstation (Metrohm China Ltd.) was employed for electrochemical studies. All the experiments were carried out with a three-electrode system including a glassy carbon electrode (GCE, 3 mm diameter) as a working electrode, a platinum pole electrode as an auxiliary and an Ag/AgCl electrode as a reference electrode. UV–visible spectrum was obtained by an UV–visible spectrophotometer (Ls55, Perkin Elmer Instruments, America). Powder X-ray diffraction (XRD) was carried out with a X-ray diffractometer (Ultima lti Rigaku Corporation, Japan). Field emission scanning electron microscopes (SEM) (SUPPRA 55 sapphire, German Carl ZESS, German) and transmission electron microscope (TEM) (Tecnai G20, FEI, America) were applied for observing the exterior and interior morphologies of synthetic materials.

2.3. Synthesis of 3D graphene

Graphene oxide (GO) was synthesized according to the modified Hummers' method [43]. Firstly, graphite powder (3.0 g), concentrated sulfuric acid (70 mL) and sodium nitrate (1.5 g) were mixed under an ice bath under stirring. Then $KMnO_4$ (9.0 g) was slowly added and the temperature was maintained below 20 °C. Next, the reaction was transferred to water bath at 35–40 °C and maintained for 0.5 h to form a thick paste. After that, water (140 mL) was added and the temperature was increased to 98 °C, and stirred for 40 min. Successively, 70 mL water was added to terminate reaction. Then, H_2O_2 was slowly added into the mixture until the color of the solution changed from brown to yellow. The yellow GO dispersion was filtered and washed with 1 M HCl aqueous solution and water repeatedly to remove the residuals. Secondly, 3D graphene was prepared by heating homogeneous GO aqueous dispersion (2 mg mL^{-1}) in a Teflon-lined autoclave at 180 °C for 12 h [44]. In order to improve the dispersion stability of 3D graphene, Nafion solution (5 wt%) was added in the 3D graphene aqueous solution (2 mg mL^{-1}).

2.4. Synthesis of Cu_2O -MWCNTs

In a typical synthesis [45], 40 mL H_2O and 1 mL sodium citrate (0.36 M) was mixed at 32 °C under vigorous stirring. After 20 min, 1 mL $CuSO_4 \cdot 5H_2O$ (1.2 M) solution was quickly added, followed by 1 mL NaOH (4.8 M) solution and held for 5 min. Then, 1 mL ascorbic acid (1.2 M) was injected and the reaction was maintained for 30 min. The product was washed with water and alcohol three times and dried.

Appropriate amount of MWCNTs was added into the mix acids H_2SO_4/HNO_3 (3:1) and ultrasonicated for 24 h to get –COOH functional groups. Then the mixture was thoroughly rinsed with water to remove residual acids. The carboxylated MWCNTs was dried and dispersed in ethanol (1 mg mL^{-1}). Next, the Cu_2O was mixed with the MWCNTs alcoholic solution, the mixture was sonicated to a well-distributed solution. The final product was obtained after washed with deionized water and ethanol several times and centrifuged.

2.5. Synthesis of RuSi NPs

$Ru(bpy)_3^{2+}$-doped silica nanoparticles were synthesized according to the previous report [46]. In brief, TX-100 (1.77 mL), cyclohexane (7.5 mL), 1-hexanol (1.8 mL), water (340 μL) and $Ru(bpy)_3^{2+}$ aqueous solution (0.1 M, 80 μL) were mixed. In the presence of TEOS (100 μL), the reaction was initiated by adding $NH_3 \cdot H_2O$ and completed after stirring for 24 h. Acetone was used to isolate the precipitate, followed by centrifuging and washing with ethanol and water for several times. The obtained RuSi NPs were

dispersed in ethanol (3 mg mL^{-1}) and added nafion (5 wt%) to improve the dispersion stability, the solution was stored at 4 °C.

2.6. Fabrication of ECL aptasensor

The aptasensor was fabricated by the following steps (Scheme 1). First, the GCE was polished with 0.3 and 0.05 μm alumina powder sequentially, then washed with distilled water and sonicated in distilled water, ethanol, respectively, and dried at room temperature. And then, the cleaned electrode was coated with a certain amount of the as-prepared 3D graphene (2 mg mL^{-1}) and dried at room temperature. Next, Cu_2O-MWCNTs (1 mg mL^{-1}) were dropped onto the surface of 3D graphene and dried at the room temperature. 5 μL aqueous solution containing EDC (20 nM) and NHS (10 mM) was added onto the nanomaterials modified electrode, and then dried at room temperature for 1 h. Finally, the electrode was washed with deionized water to remove the remainder.

The thrombin aptamers were prepared with Tris-HCl (50 mM, pH 7.4) buffer solution before using, and then the electrode was soaked into 1 mL BSA solution (1 μM) for 12 h at 4 °C to block unbound sites on the electrode surface, 5 μL of SMCC solution was dropped onto the surface to link the RuSi NPs. The electrode was washed carefully with Tris-HCl buffer solution (pH 7.4) every step to remove the nonspecifically bound substance. Thereafter, 5 μL sample solution containing different concentration of thrombin was placed on the electrode and incubated at 37 °C for 1 h, and finally washed with Tris-HCl (pH 7.4) to remove the remainder.

2.7. Measurement procedures

ECL measurements were carried out at a photomultiplier tube voltage of 800 V and a scanning rate of 100 mV s^{-1} in PBS (pH 7.4) solution.

3. Results and discussion

3.1. Characterization of 3D graphene, Cu_2O -MWCNTs and $Ru(bpy)_3^{2+}$-doped silica

The exterior and interior morphologies of the as-prepared 3D graphene were investigated by SEM (Fig. 1A) and TEM (Fig. 1B). The 3D graphene had many wrinkles and ripples, the partial overlapping and staking of graphene sheets which resulted in high surface area that enhanced the loading property of graphene.

As shown in Fig. 1C, the Cu_2O nanoparticles mixed with MWCNTs presented nanocubes in uniform shape with edge lengths about 60 nm. Fig. 1D shows the XRD pattern of the Cu_2O-MWCNTs. The peak value of 26.0 corresponds to the characteristic peak of (002) of MWCNTs, and three peaks value at 36.5, 42.4 and 61.5 corresponds to (111), (200) and (220) crystal planes of pure Cu_2O nanoparticles, respectively [40,47]. This result indicates that the as-prepared materials were composed of Cu_2O and MWCNTs.

As shown in Fig. 1E, the RuSi NPs were spherical nano-particles which were homogeneous in formation and the diameter was about 50 nm. The EDX (Fig. 1F) shows the RuSi NPs contained elements of Si and Ru.

3.2. Characterization of the modified electrode

Fig. 2 shows ECL-time curves of GCE modified by (a) 3D graphene/Cu_2O-MWCNTs/TBA/RuSiNPs, (b) Cu_2O-MWCNTs/TBA/RuSi NPs, (c) 3D graphene/RuSi NPs, (d) RuSi NPs in PBS (pH 7.4) with 1 pM thrombin. Comparison of ***curve a*** and ***curve b***, 3D graphene/Cu_2O-MWCNTs/TBA/RuSi NPs modified electrode exhibited much higher ECL intensity than Cu_2O-MWCNTs/TBA/RuSi NPs modified electrode which indicated that the large specific surface area and high electrical conductivity of 3D graphene could improve ECL intensity. Compare with ***curve c***, ***curve a*** showed higher ECL signals. It illustrated that the presence of thrombin made the TBA forming a G-quadruplex conformation and leading RuSi NPs got closer to

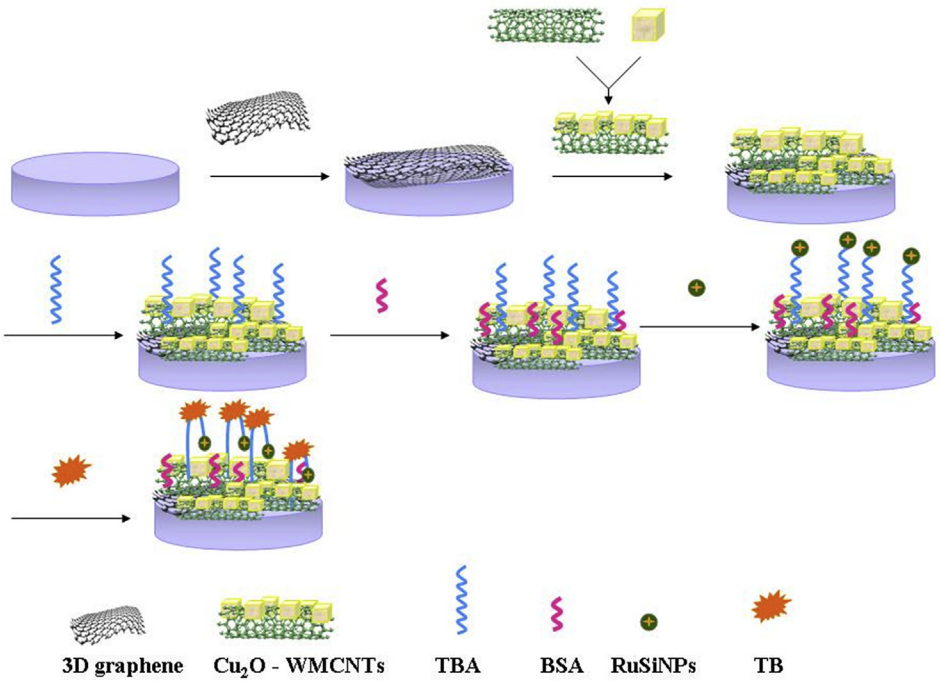

Scheme 1. Illustration of the preparation procedures for the ECL aptasensor.

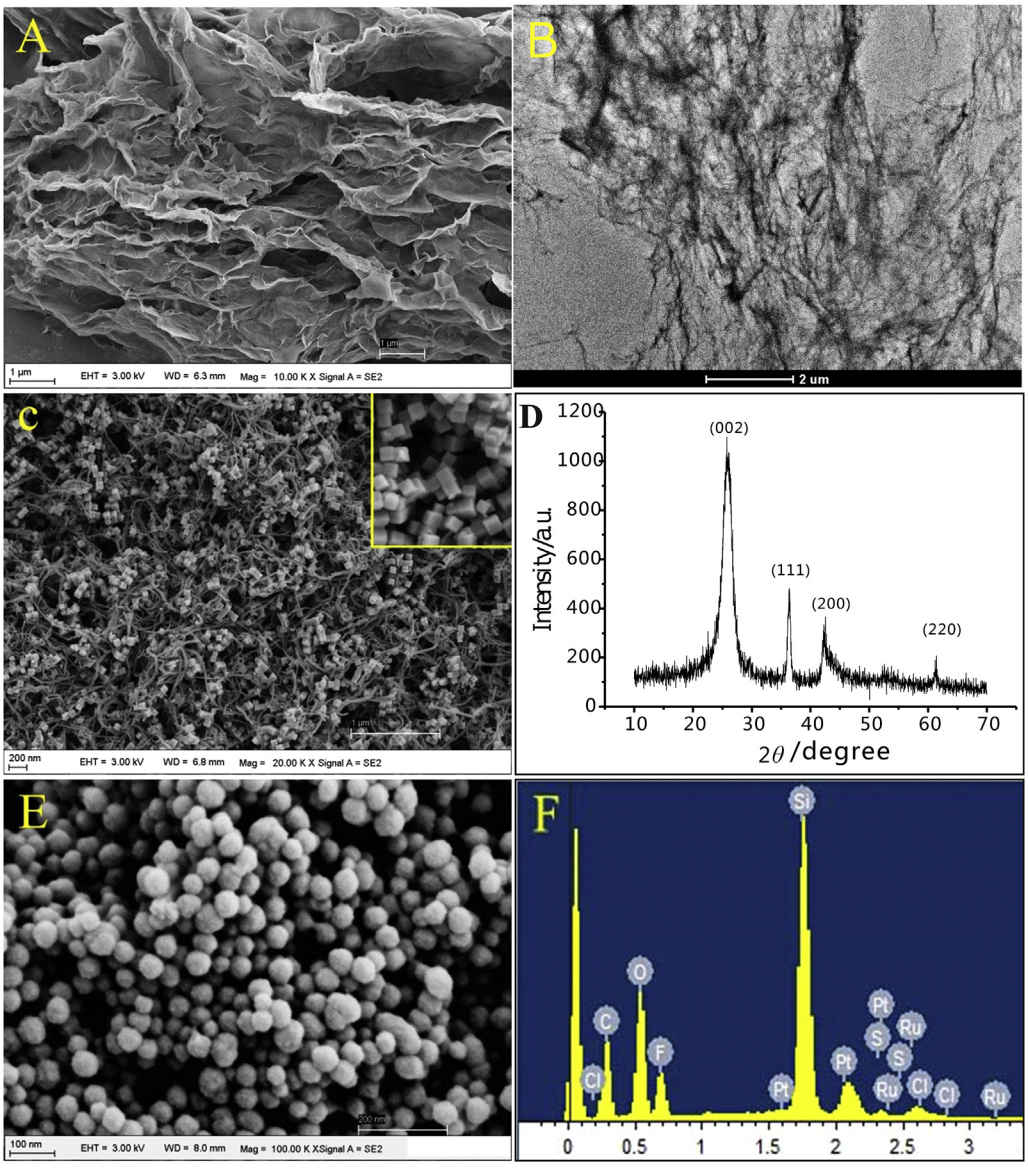

Fig. 1. SEM (A) and TEM (B) images of 3D graphene. SEM image(C) and XRD (D) of Cu_2O-MWCNTs (The inset of C is SEM image of Cu_2O). SEM image (E) and EDX (F) of RuSi NPs.

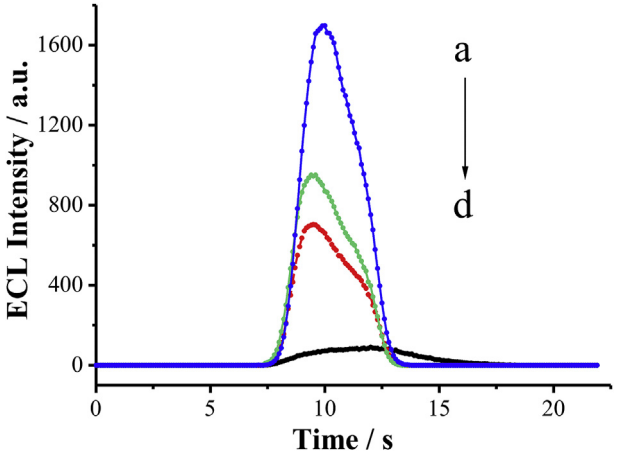

Fig. 2. ECL-time curves of (a) 3D graphene/Cu_2O-MWCNTs/TBA/RuSi NPs, (b) Cu_2O-MWCNTs/TBA/RuSi NPs, (c) 3D graphene/RuSi NPs, (d) RuSi NPs in PBS (pH 7.4) with 1.0×10^{-12} M TB.

Cu_2O, at the same time, the cyclic catalyzed function enhanced the ECL intensity and specific detected thrombin. ***Curve d*** presented the lowest ECL intensity, which indicated the modification of 3D graphene and Cu_2O-MWCNTs could enhance the ECL intensity. Thus, 3D graphene/Cu_2O-MWCNTs/TBA/RuSi NPs modified film presented both the advantages of 3D graphene and Cu_2O-MWCNTs, making significant enhance the ECL signal.

Fig. 3 shows the electrochemical impedance spectroscopy (EIS) of each modified electrode. The EIS of bare GCE electrode (***curve a***) was almost a line at low alternating current (AC) modulation frequency and presented a hemicycle at high AC modulation frequency, indicating that GCE electrode was controlled by diffusion at low frequency and by electron transfer at high frequency. As shown in the insert, compared with ***curve a***, ***curve b*** and ***curve c*** were almost straight lines indicated that 3D graphene or Cu_2O-MWCNTs modified electrodes could greatly accelerate electron transfer, so the modified electrode presented smaller R_{ct}. R_{ct} increased after TBA was absorbed on the electrode due to the insulating property of DNA (***curve d***, ***curve e***). TB is a protein, would also inhibit interfacial

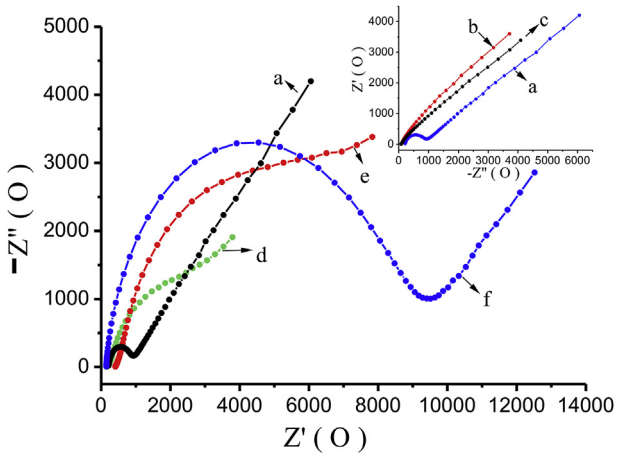

Fig. 3. EIS Nyquist of the (a) bare GCE and (b) 3D graphene, (c) Cu_2O-MWCNTs, (d) 3D graphene/Cu_2O-MWCNTs/TBA, (e) Cu_2O-MWCNTs/TBA, (f) 3D graphene/Cu_2O-MWCNTs/TBA/RuSi NPs modified electrode in a 1:1 mixture of 5 mM $K_3[Fe(CN)_6]$/$K_4[Fe(CN)_6]$ and 0.1 M KCl aqueous solution.

charge transfer, so the R_{ct} increased. At last, the R_{ct} increased again because SiO_2 is insulating (***curve f***).

3.3. Optimization of experimental parameters

Some key factors influencing the ECL response were investigated, including the amount of 3D graphene, the amount of Cu_2O-MWCNTs and the concentration of TBA.

Fig. 4A shows the relationship between the amount of 3D graphene and ECL intensity. ECL intensity increased with the amount of 3D graphene ranging from 7.0 to 13.0 μg, and decreased at higher amount. It could be explained that 3D graphene could enhance the ECL intensity by accelerating electron transport, but the dark colored graphene presented negative effect on the ECL intensity. Therefore, the optimal amount of 3D graphene was 10.0 μg.

As shown in Fig. 4B, the ECL intensity increased with increasing the amount of Cu_2O-MWCNTs but was followed by a decrease while the amount was larger than 4.0 μg. Because the amount of Cu_2O-MWCNTs increased, the cyclic catalysis was activated to improve the ECL intensity. However, the light signal emitted by $Ru(bpy)_3^{2+}$ might be absorbed by Cu_2O and the thick film may hinder the ECL signal. Hence, 4.0 μg Cu_2O-MWCNTs was chosen for further experiment.

In order to obtain the optimal incubate concentration of TBA, the UV–vis absorption of TBA solution was measured before and after incubated (Fig. 4C). The inset figure shows the characteristic UV absorption peak of TBA is 260 nm. When the electrode was incubated in 0.1 nM, 1 nM, or 10 nM aptamer solutions, the UV absorption significantly decreased after incubating, indicating that all of the aptamers were successfully absorbed on the electrode. When the electrode was incubated in 100 nM aptamer solution, the UV absorption that after incubated was higher than that of 0.1 nM, 1 nM or 10 nM aptamer solution, which indicates that 100 nM aptamer exceed the absorptive amount of the electrode. Hence, to ensure enough aptamers were absorbed on the electrode, 1 μM TBA that tenfold excess concentration was chosen.

3.4. Mechanism of the ECL aptasensor

The redox reaction of $Ru(bpy)_3^{2+}$ occurs by applying appropriate voltage (0.2–1.25 V) to the electrode through cyclic voltammetry (CV), when only RuSiNPs were fabricated on the electrode, weak emission was obtained (Fig. 2, *curve d*), the ECL can be assigned to the anodic ECL reactions between the low concentration of OH^- in PBS and $Ru(bpy)_3^{2+}$ on the electrode (see eqs. (1)–(3)) [48].

$$Ru(bpy)_3^{2+} - e^- \rightarrow Ru(bpy)_3^{3+} \quad (1)$$

$$Ru(bpy)_3^{3+} + OH^- \rightarrow [Ru(bpy)_3^{2+}]^* + 1/2H_2O + 1/4O_2 \quad (2)$$

$$[Ru(bpy)_3^{2+}]^* \rightarrow Ru(bpy)_3^{2+} + h\nu \text{ luminescence} \quad (3)$$

$$Cu_2O + h\nu \rightarrow h^+ + e^- \text{ photocatalytic} \quad (4)$$

$$h^+ + OH^- \rightarrow \cdot OH \quad (5)$$

$$Ru(bpy)_3^{2+} + \cdot OH \rightarrow Ru(bpy)_3^{3+} \quad (6)$$

$$O_2 + e^- \rightarrow O_2\cdot^- \quad (7)$$

$$Ru(bpy)_3^{3+} + O_2\cdot^- \rightarrow [Ru(bpy)_3^{2+}]^* + O_2 \quad (8)$$

Cu_2O, as a photocatalytic material, can be excited by light of wavelength at 400–800 nm and produced electrons (e^-) and holes (h^+) (eq. (4)). In Fig. 5, Cu_2O had a wide adsorption range and the maximum adsorption wavelength was 482 nm and the adsorption, the fluorescence emission of $Ru(bpy)_3^{2+}$ was at 610 nm, the emission light of $Ru(bpy)_3^{2+}$ can excite the Cu_2O. Under light excitation, the generated electrons in p-type semiconductor Cu_2O are captured by electron acceptors (dissolved O_2), and the generated holes have strong oxidizability to electron donors [49,50]. So the holes can combine with OH^- to generate intermediate ·OH (eq. (5)) which can react with $Ru(bpy)_3^{2+}$ and produced more $Ru(bpy)_3^{3+}$ (eq. (6)); the electrons can combine with the dissolved O_2 and generated strongly reducing intermediate $O_2\cdot^-$ (eq. (7)), the chemical reduction of $Ru(bpy)_3^{3+}$ by the strongly reducing $O_2^{\bullet-}$ to produce the excited state $[Ru(bpy)_3^{2+}]^*$ (eq. (8)) [48]. In conclusion, the light

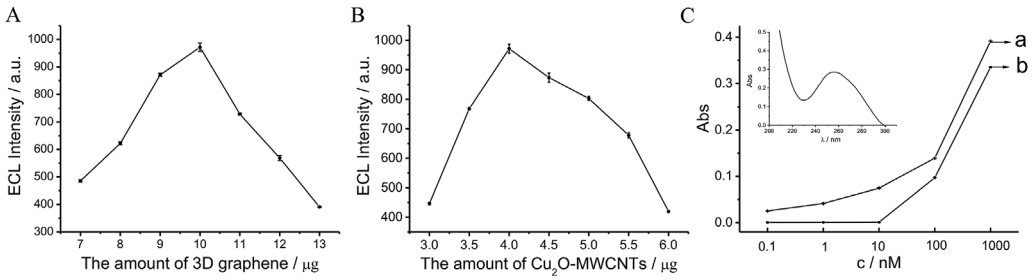

Fig. 4. Effects of (A) the amount of 3D graphene, (B) the amount of Cu_2O-MWCNTs on the ECL intensity in phosphate buffer (pH 7.4) with 1.0×10^{-13} M TB, (C) the UV–vis absorption of TBA at 260 nm before and after incubated The inset of (C) is the UV absorption spectra of 1 μM TBA.

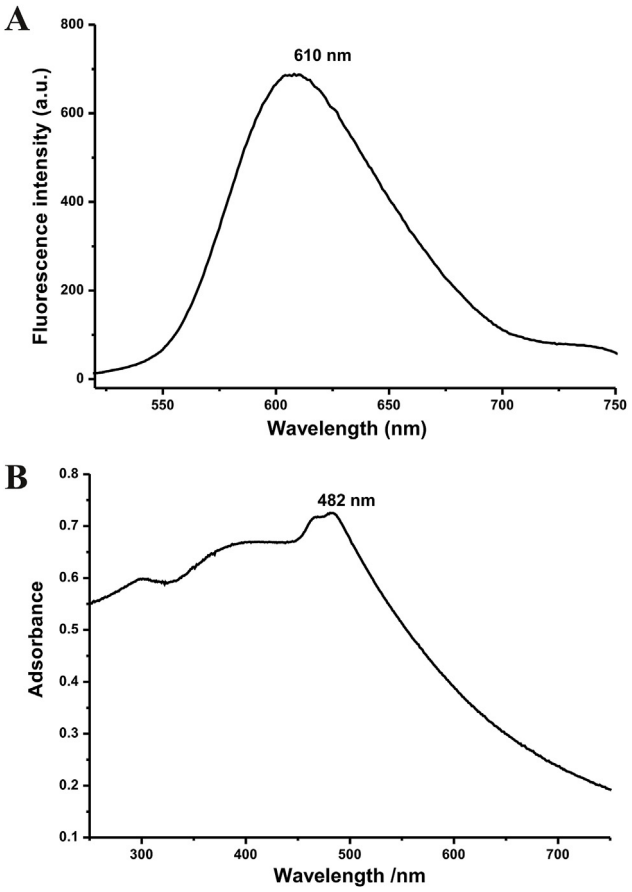

Fig. 5. (A) The fluorescence spectra of RuSiNPs; (B) the UV–Vis adsorption spectra of Cu_2O.

generated from $Ru(bpy)_3^{2+}$ redox reaction can motivate photocatalytic material Cu_2O, and Cu_2O can catalyze redox reaction of $Ru(bpy)_3^{2+}$ to emit more light. Therefore, a cyclic catalysis ECL aptasensor is built.

3.5. Determination of thrombin

On the basis of the optimal conditions, the ECL sensor was constructed for sensitive determination of TB. As shown in Fig. 5, the ECL intensity (I) exhibits a linear response to the logarithmic TB concentration ranging from 5.0×10^{-15} to 5.0×10^{-11} M with a correlation coefficient of 0.9997, the calibration curve was $I = 606.7 \times \log C_{TB} + 8876.1$ (mol L^{-1}), and the detection limit (S/N = 3) is 1.3×10^{-15} M. The inset shows the ECL emission of ten continuous circles.

While comparing the analytical performance of this aptasensor with other modified electrodes methods for the detection of TB by ECL method (Table 1), this method presents lower detection limit and wider linear range.

3.6. Repeatability, stability and interference test

Excellent repeatability and stability are important characters for a sensor. In this work, the relative standard deviation (RSD) for ten successive measurements of the same sensor is 4.0%, and RSD for eight different electrodes constructed in the same way is 1.1%. Additionally, the stability was tested by detecting TB solution at different time slots. The modified electrodes were stored 4 °C while not use it. The result indicates that the ECL intensity maintained 94.0%~96.3% of the original response after 15 days. Therefore, the sensor presented good repeatability and stability.

The tolerant maximum concentration of the coexistent was investigated, including BSA (10^{-12} M), IgG (10^{-12} M), BHb (10^{-12} M), and the mixture in TB (2.5×10^{-13} M). According to Fig. 6, BSA, IgG and BHb were poorly response to the sensor, and the ECL signal of mix sample (compose of 10^{-12} M of BSA, IgG, BHb and 2.5×10^{-13} M of TB) was almost equal to the signal response to only TB. The results show that the developed aptasensor presented high selectivity for detection of TB (see Fig. 7).

4. Conclusions

In summary, this work demonstrates an ultrasensitive ECL aptasensor based on the 3D graphene/Cu_2O-MWCNTs/TBA/RuSi NPs modified electrode. Photocatalytic material Cu_2O was introduced to build a cyclic catalytic system to improve the ECL intensity. In addition, 3D graphene and MWCNTs were used to accelerate the electron transfer, thus further improved the ECL intensity. Benefiting from the sensitivity, stability, specificity, good repeatability and low detection limit, the developed aptasensor shows

Table 1
Comparisons of analytical performance of this work with the other different modified electrodes methods for the determination of thrombin by ECL method.

Modified material	Electrode	Linear range (mol L^{-1})	Detection limit (mol L^{-1})	Reference
Cu_2O@aptamer	Gold electrode	3.3×10^{-12} -1.6×10^{-9}	3.3×10^{-13}	[28]
Bifunctional aptamer/N-(aminobutyl)-N-(ethylisoluminol) functionalized gold nanoparticles	Gold electrode	5.0×10^{-14} -5.0×10^{-10}	1.2×10^{-14}	[29]
Ferrocene-graphene nanosheets/$Ru(bpy)_3^{2+}$ tagged aptamer	Glassy carbon electrode	5.0×10^{-10} -2.5×10^{-8}	2.1×10^{-10}	[30]
Ferrocene-labeled ligand-bound aptamer molecular beacon	Glassy carbon electrode	5.0×10^{-12} -5.0×10^{-8}	1.7×10^{-12}	[31]
Tris(bipyridine)ruthenium(II)-β-cyclodextrin/aptamer	Glassy carbon electrode	1.0×10^{-12} -1.0×10^{-8}	1.0×10^{-13}	[32]
$Ru(bpy)_3^{2+}$/three-Layer Porous Fe_3O_4@SiO_2@Au Nanoparticles	Glassy carbon electrode	1.0×10^{-8}~1.0×10^{-5}	3.0×10^{-15}	[33]
graphene/hemin/gold nanorods/Gquadruplex–hemin/quantum dots	Glassy carbon electrode	1.0×10^{-4}~5.0×10^{-10}	4.2×10^{-12}	[34]
silver nanoclusters/DNAzyme-assisted target	Gold electrode	1.0×10^{-14} -1.0×10^{-8}	4.5×10^{-15}	[35]
3D graphene/Cu_2O-MWCNTs/RuSiNPs	Glassy carbon electrode	5.0×10^{-15} -5.0×10^{-11}	1.3×10^{-15}	This work

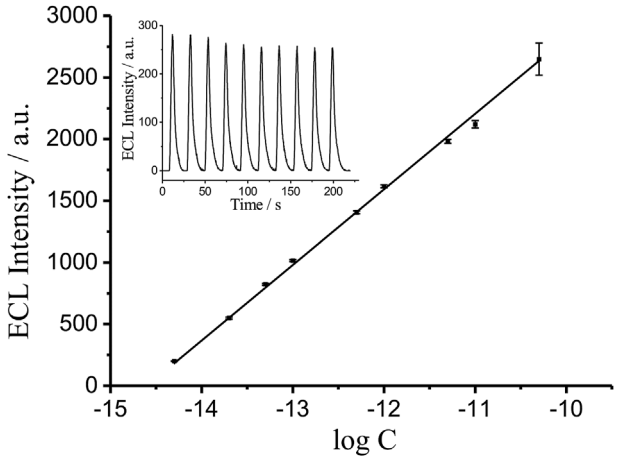

Fig. 6. Calibration curve of ECL intensity to logarithmic TB concentration. The inset shows the ECL emission under ten continuous circles.

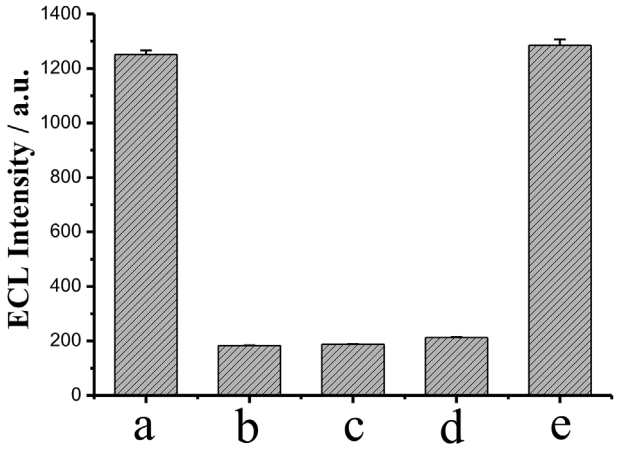

Fig. 7. ECL responses of the aptasensor for (a) 2.5×10^{-13} M of thrombin, 10^{-12} M of (b) BSA, (c) IgG, (d) BHb and (e) their mixture.

great promising for detection of TB and has a wide potential application in bioanalysis.

Acknowledgments

The project was supported by the National Natural Science Foundation of China (Nos. 21365004, 21065001, 21165003), Guangxi Natural Science Foundation (Nos. 2013GXNSFDA019006, 2016GXNSFBA380201), Scientific Research Fund of Guangxi Education Department (Nos. 2013ZD019), Fundamental Research Fund for the Guangxi University for Nationalities (2015MDQD011).

References

[1] D.L. Robertson, G.F. Joyce, Selection in vitro of an RNA enzyme that specifically cleaves single-stranded DNA, Nature 344 (1990) 467–468.
[2] A.D. Ellington, J.W. Szostak, In vitro selection of RNA molecules that bind specific ligands, Nature 346 (1990) 818–822.
[3] M. Famulok, G. Mayer, M. Blind, Nucleic acid aptamers from selection in vitro to applications in vivo, Acc. Chem. Res. 33 (2000) 591–599.
[4] H.R. Zhang, M.S. Wu, J.J. Xu, H.Y. Chen, Signal-on dual-potential electrochemiluminescence based on luminol-gold bifunctional nanoparticles for telomerase detection, Anal. Chem. 86 (2014) 3834–3840.
[5] D.F. Wang, Y.Y. Li, Z.Y. Lin, B. Qiu, L.H. Guo, Surface-enhanced electrochemiluminescence of Ru@SiO_2 for ultrasensitive detection of carcinoembryonic antigen, Anal. Chem. 87 (2015) 5966–5972.
[6] D. Jie, Z.H. Guo, X.W. Zheng, Label-Free sensitive electrogenerated chemiluminescence aptasensing based on chitosan/$Ru(bpy)_3^{2+}$/silica nanoparticles modified electrode, Anal. Chem. 86 (2014) 8943–8950.
[7] Y.L. Luo, J.Y. Xu, Y. Li, H.T. Gao, J.J. Guo, F. Shen, C.Y. Sun, A novel colorimetric aptasensor using cysteamine-stabilized gold nanoparticles as probe for rapid and specific detection of tetracycline in raw milk, Food Control 54 (2015) 7–15.
[8] M. Ramezani, N.M. Danesh, P. Lavaee, K. Abnous, S.M. Taghdisi, A novel colorimetric triple-helix molecular switch aptasensor for ultrasensitive detection of tetracycline, Biosens. Bioelectron. 70 (2015) 181–187.
[9] M. Mir, M. Vreeke, I. Katakis, Different strategies to develop an electrochemical thrombin aptasensor, Electrochem. Commun. 8 (2006) 505–511.
[10] A.X. Zheng, J.R. Wang, J. Li, X.R. Song, G.N. Chen, H.H. Yang, Enzyme-free fluorescence aptasensor for amplification detection of human thrombin via target-catalyzed hairpin assembly, Biosens. Bioelectron. 36 (2012) 217–221.
[11] Z.H. Zhang, S. Zhang, S.L. Liu, M.H. Wang, G.D. Fu, L.H. He, Y.Q. Yang, S.M. Fang, Electrochemical aptasensor based on one-step synthesis of Cu_2O@aptamer nanospheres for sensitive thrombin detection, Sens. Actuators, B 220 (2015) 184–191.
[12] W. Dan, X. Xia, X.H. Pang, M. Pietraszkiewicz, R. Hozyst, X.G. Sun, Q. Wei, Application of eu-multi-walled carbon nanotubes as a novel luminophore in electrochemiluminescent aptasensor for thrombin using multiple amplification strategies, ACS Appl. Mater. Interfaces 7 (2015) 12663–12670.
[13] D.F. Wang, Y.Y. Li, Z.Y. Lin, B. Qiu, L.H. Guo, Surface-enhanced electrochemiluminescence of Ru@SiO_2 for ultrasensitive detection of carcinoembryonic antigen, Anal. Chem. 87 (2015) 5966–5972.
[14] M.M. Richter, Electrochemiluminescence (ECL), Chem. Rev. 104 (2004) 3003–3036.
[15] J.T. Cao, J.J. Yang, L.Z. Zhao, Y.L. Wang, H. Wang, Y.M. Liu, S.H. Ma, Graphene oxide@gold nanorods-based multiple-assisted electrochemiluminescence signal amplification strategy for sensitive detection of prostate specific antigen, Biosens. Bioelectron. 99 (2018) 92–98.
[16] Y.L. Wang, F.R. Liu, J.T. Cao, S.W. Ren, Y.M. Liu, Spatial-resolved dual-signal-output electrochemiluminescent ratiometric strategy for accurate and sensitive immunoassay, Biosens. Bioelectron. 102 (2018) 525–530.
[17] D. Jiang, X.J. Du, Q. Liu, N. Hao, J. Qian, L.M. Dai, H.P. Mao, K. Wang, Anchoring AgBr nanoparticles on nitrogen-doped graphene for enhancement of electrochemiluminescence and radical stability, Chem. Commun. 51 (2015) 4451–4454.
[18] X.J. Du, D. Jiang, L.M. Dai, W.R. Zhu, X.D. Yang, N. Hao, K. Wang, Oxygen vacancy engineering in europia clusters/graphite-like carbon nitride nanostructures induced signal amplification for highly efficient electrochemiluminesce aptasensing, Anal. Chem. 90 (2018) 3615–3620.
[19] X.J. Du, D. Jiang, N. Hao, J. Qian, L.M. Dai, L. Zhou, J.P. Hu, K. Wang, Building a three-dimensional Nano–Bio interface for aptasensing: an analytical methodology based on steric hindrance initiated signal amplification effect, Anal. Chem. 88 (2016) 9622–9629.
[20] H. Wei, E.K. Wang, Solid-state electrochemiluminescence of tris(2,2′-bipyridyl) ruthenium, TrAC, Trends Anal. Chem. 27 (2008) 447–459.
[21] Y.H. Liao, X.M. Zhou, Y. Fu, D. Xing, Linear $Ru(bpy)_3^{2+}$-Polymer as a universal probe for sensitive detection of biomarkers with controllable electrochemiluminescence signal-amplifying ratio, Anal. Chem. 89 (2017) 13016–13023.
[22] F.K. Du, H. Zhang, X.C. Tan, J. Yan, M. Liu, X. Chen, Y.Y. Wu, et al., $Ru(bpy)_3^{2+}$-Silica@Poly-L-lysine-Au as labels for electrochemiluminescence lysozyme aptasensor based on 3D graphene, Biosens. Bioelectron. 86 (2018) 50–56.
[23] H. Ke, H.F. Sha, Y.F. Wang, W.W. Guo, X. Zhang, Z.M. Wang, C.S. Huang, N.Q. Jia, Electrochemiluminescence resonance energy transfer system between GNRs and $Ru(bpy)_3^{2+}$: application in magnetic aptasensor for β-amyloid, Biosens. Bioelectron. 100 (2018) 266–273.
[24] W. Zhang, H.W. Xiong, M.M. Chen, X.H. Zhang, S.F. Wang, Surface-enhanced molecularly imprinted electrochemiluminescence sensor based on Ru@SiO_2 for ultrasensitive detection of fumonisin B1, Biosens. Bioelectron. 96 (2017) 55–61.
[25] X.Y. Wang, Y.J. Wang, M. Jiang, Y.Q. Shan, X. Jin, M. Gong, X.N. Wang, Functional electrospun nanofibers-based electrochemiluminescence immunosensor for detection of the TSP_{53} using RuAg/SiO_2NPs as signal enhancers, Anal. Biochem. 548 (2018) 15–22.
[26] M. Mir, M. Vreeke, I. Katakis, Different strategies to develop an electrochemical thrombin aptasensor, Electrochem. Commun. 8 (2006) 505–511.
[27] B. Deng, Y.W. Lin, C. Wang, F. Li, Z.X. Wang, H.Q. Zhang, X.F. Li, X.C. Le, Aptamer binding assays for proteins: the thrombin example—a review, Anal. Chim. Acta 837 (2014) 1–15.
[28] Z.H. Zhang, S. Zhang, S.L. Liu, M.H. Wang, G.D. Fu, L.H. He, Y.Q. Yan, S.M. Fang, Electrochemical aptasensor based on one-step synthesis of Cu_2O@aptamer nanospheres for sensitive thrombin detection, Sens. Actuators B Chem. 220 (2015) 184–191.
[29] C. Ying, D. Tian, C. Hua, Electrochemiluminescence biosensor for the assay of small molecule and protein based on bifunctional aptamer and chemiluminescent functionalized gold nanoparticles, Anal. Chim. Acta 715 (2012) 86–92.
[30] B. Zhuo, Y. Li, X. Huang, Y. Lin, Y. Chen, W. Gao, An electrochemiluminescence aptasensing platform based on ferrocene-graphene nanosheets for simple and rapid detection of thrombin, Sens. Actuators B Chem. 208 (2015) 518–524.
[31] Y.H. Liao, R. Yuan, Y.Q. Chai, L. Mao, Y. Zhuo, Y.L. Yuan, L.J. Bai, S.R. Yuan, Electrochemiluminescence quenching via capture of ferrocene-labeled ligand-

bound aptamer molecular beacon for ultrasensitive detection of thrombin, Sens. Actuators B Chem. 158 (2011) 393–399.
[32] Q. Chen, H. Chen, Y.Y. Zhao, F. Zhang, F. Yang, J. Tang, P.G. He, A label-free electrochemiluminescence aptasensor for thrombin detection based on host–guest recognition between tris(bipyridine)ruthenium(ii)-β-cyclodextrin and aptamer, Biosens. Bioelectron. 54 (2014) 547–552.
[33] L.R. Hong, J. Zhao, Y.M. Lei, R. Yuan, Y. Zhuo, Efficient electrochemiluminescence from $Ru(bpy)_3^{2+}$ enhanced by three-Layer porous Fe_3O_4 @SnO_2 @Au nanoparticles for label-free and sensitive bioanalysis, Electrochim. Acta 241 (2017) 291–298.
[34] K. Shao, B.R. Wang, S.Y. Ye, Y.P. Zuo, L. Wu, Q. Li, Z.C. Lu, X.C. Tan, H.Y. Han, Signal-amplified near-infrared ratiometric electrochemiluminescence aptasensor based on multiple quenching and enhancement effect of graphene/gold nanorods/G-quadruplex, Anal. Chem. 88 (2017) 8179–8187.
[35] G.F. Jie, L. Tan, Y. Zhao, X.C. Wang, A novel silver nanocluster in situ synthesized as versatile probe for electrochemiluminescence and electrochemical detection of thrombin by multiple signal amplification strategy, Biosens. Bioelectron. 94 (2017) 243–249.
[36] A.E. Rakhshani, Preparation, characteristics and photovoltaic properties of cuprous oxide—a review, Solid State Electron. 29 (1986) 7–17.
[37] L.L. Wang, J. Ge, A.L. Wang, M.S. Deng, X.J. Wang, S. Bai, R. Li, J. Jiang, Q. Zhang, Y. Luo, Y.J. Xiong, Designing p-type semiconductor-metal hybrid structures for improved photocatalysis, Angew. Chem. Int. Ed. 53 (2014) 5207–5211.
[38] L.S. Zhang, J. Li, Z. Chen, Y. Tang, Y. Yu, Preparation of fenton reagent with H_2O_2 generated by solar light-illuminated nano-Cu_2O/MWNTs composites, Appl. Catal. A 299 (2006) 292–297.
[39] P.J. Britto, K.S.V. Santhanam, R. Angel, J.A. Alonso, P.M. Ajayan, Improved charge transfer at carbon nanotube electrodes, Adv. Mater. 11 (1999) 154–157.
[40] W.W. Li, S. Gao, L.Q. Wu, S.Q. Qiu, Y.F. Guo, X.M. Geng, M.L. Chen, S.T. Liao, C. Zhu, Y.P. Gong, M.S. Long, J.B. Xu, X.F. Wei, M.T. Sun, L.W. Liu, High-density three-dimension graphene macroscopic objects for high-capacity removal of heavy metal ions, Sci. Rep. 3 (2013), 120-120.
[41] X. Huang, Z.Y. Yin, S.X. Wu, X.Y. Qi, Q.Y. He, Q.C. Zhang, Q.Y. Yan, F. Boey, H. Zhang, Graphene-based materials: synthesis, characterization, properties, and applications, Small 7 (2011) 1876–1902.
[42] C. Li, G.Q. Shi, Three-dimensional graphene architectures, Nanoscale 4 (2012) 5549–5563.
[43] Y.X. Xu, Z.Y. Lin, X.Q. Huang, Y. Wang, Y. Huang, X.F. Duan, Functionalized graphene hydrogel-based high-performance supercapacitors, Adv. Mater. 25 (2013) 5779–5784.
[44] Y.X. Xu, K.X. Sheng, C. Li, G.Q. Shi, Self-assembled graphene hydrogel via a one-step hydrothermal process, ACS Nano 4 (2010) 4324–4330.
[45] I.C. Chang, P.C. Chen, M.C. Tsai, T.T. Chen, M.H. Yang, H.T. Chiu, C.Y. Lee, Large-scale synthesis of uniform Cu_2O nanocubes with tunable sizes by in-situ nucleation, Crystengcomm 15 (2013) 2363–2366.
[46] L.H. Zhang, S.J. Dong, Electrogenerated chemiluminescence sensors using $Ru(bpy)_3^{2+}$ doped in silica nanoparticles, Anal. Chem. 78 (2006) 5119–5123.
[47] S. Kakuta, T. Abe, A novel example of molecular hydrogen generation from formic Acid at visible-light-responsive photocatalyst, ACS Appl. Mater. Interfaces 1 (2009) 2707–2710.
[48] L.Y. Zheng, Y.W. Chi, Q.Q. Shu, Y.Q. Dong, L. Zhang, G.N. Chen, Electrochemiluminescent reaction between $Ru(bpy)_3^{2+}$ and oxygen in nafion film, J. Phys. Chem. C 113 (2009) 20316–20321.
[49] G.L. Wang, J.X. Shu, Y.M. Dong, X.M. Wu, W.W. Zhao, J.J. Xu, H.Y. Chen, Using g-quadruplex/hemin to “Switch-On” the cathodic photocurrent of p-type PbS quantum dots: toward a versatile platform for photoelectrochemical aptasensing, Anal. Chem. 87 (2015) 2892–2900.
[50] G.C. Fan, H. Zhu, D. Du, J.R. Zhang, J.J. Zhu, Y.H. Lin, Enhanced photoelectrochemical immunosensing platform based on CdSeTe@CdS:Mn Core–Shell quantum dots-sensitized TiO_2 amplified by CuS nanocrystals conjugated signal antibodies, Anal. Chem. 88 (2016) 3392–3399.